Molecular Crystals and Liquid Crystals

ISSN: 1542-1406 (Print) 1563-5287 (Online) Journal homepage: http://www.tandfonline.com/loi/gmcl20

Optical diffraction by using electrically-controlled spatially patterned nematic pentylcyanobiphenyl films under static electric field

Georgi B. Hadjichristov & Yordan G. Marinov

To cite this article: Georgi B. Hadjichristov & Yordan G. Marinov (2016) Optical diffraction by using electrically-controlled spatially patterned nematic pentylcyanobiphenyl films under static electric field, Molecular Crystals and Liquid Crystals, 632:1, 9-20

To link to this article: http://dx.doi.org/10.1080/15421406.2016.1185566

Published online: 17 Aug 2016.

MOLECULAR CRYSTALS AND LIQUID CRYSTALS
2016, VOL. 632, 9–20
http://dx.doi.org/10.1080/15421406.2016.1185566

Taylor & Francis
Taylor & Francis Group

Optical diffraction by using electrically-controlled spatially patterned nematic pentylcyanobiphenyl films under static electric field

Georgi B. Hadjichristov[a] and Yordan G. Marinov[b]

[a]Laboratory of Optics and Spectroscopy, Georgi Nadjakov Institute of Solid State Physics, Bulgarian Academy of Sciences, Sofia, Bulgaria; [b]Laboratory of Biomolecular Layers, Georgi Nadjakov Institute of Solid State Physics, Bulgarian Academy of Sciences, Sofia, Bulgaria

ABSTRACT

Diffractive electro-optics of electrically-induced spatially periodic texture patterns (namely, wide-formed stationary parallel stripes) in planarly-aligned films of the nematic liquid crystal 4-*n*-pentyl-4′-cyanobiphenyl (5CB) is examined under static electric field in view of its practical application. The longitudinal textural domains electrically-induced with well defined threshold and spatial period have flexo-dielectric nature and differ from the usual flexoelectric stripe distortion, as well as from the electroconvective domains of frequency-dependent morphology. The low-voltage-controlled grating effect through the flexo-dielectric domains can be useful for nematic diffractive optics.

KEYWORDS

Nematics liquid crystals; pentylcyanobiphenyls; electro-optics; optical phase grating; spatially-periodic patterned array; coherent light diffraction

1. Introduction

Various types of periodic distortions in homogeneously oriented thin layers of nematic liquid crystals (NLCs) subjected to an external electric field (alternating-current (AC) and/or direct-current (DC) electricity) have been extensively studied [1–3]. The contributions of electro-hydrodinamic, dielectric, flexoelectric and surface polarization effects to pattern formation are elaborated to great extend for both planar and homeotropic aligned layers of NLCs [4–8]. The regular field-induced spatial patterns and ordered textures in NLC materials are found to be very attractive for field-commanded effects and applications, e.g. light scattering and diffraction for use in diffractive, adaptive, active and non-linear optics, integrated optics for logic processing and optical computing, as well as in optical communication systems [9–14]. From application point of view, the employing of AC field is more favorable and attractive since in this way one can avoid various non-reversible chemical processes and electric field gradients inherent to NLCs driven with DC field. However, these unwanted effects upon static electric field applied on the NLC cells can be strongly reduced when the field magnitude is low enough.

As known, upon DC electric field or low-frequency AC field (e.g., up to 500 Hz [15]) a flexoelectric effect is possible in the NLCs, that couples the electric polarization and local director deformations in a linear way [16–18]. In particular, the influence of flexoelectricity to domain wall structure of NLC undergoing a Freedericksz transition, was studied by Elston

CONTACT Georgi B. Hadjichristov georgibh@issp.bas.bg
Color versions of one or more of the figures in the article can be found online at www.tandfonline.com/gmcl.

[19]. The region of the wall running parallel to the alignment direction was found to have a predominantly twist structure, i.e. in-plane rotation and dependance on $e_{1z}-e_{3x}$ flexoelectric coefficient difference. Whereas the wall runing perpendicular to the alignment direction exposed splay-bend structure dominated by $e_{1z}+e_{3x}$. In order to improve the performance of devices utilizing flexoelectricity in NLCs, the longitudinal domains (LDs) in planar NLCs under the joint action of AC and DC voltages have been studied [20,21].

In the research of the electrically-induced domains in planar nematics, various peculiarities of patterns formed above the Freedericksz state are not well understood. In particular, this concerns the formation of patterns with no well defined threshold shown in a sector in the low-voltage region in the morphological phase diagram given by Aguirre et al. [22] for texture patterns formed in planar NLC cells under the joint action of DC and AC electric fields. Since this region is of great practical interest, we undertook an inspection of the formation of corresponding patterns.

Recently, the electrically-induced textures in the room-temperature NLC 4-*n*-pentyl-4′-cyanobiphenyl (abbreviated as 5CB), a compound having significant dielectric and conductive anisotropy (both positive), were thoroughly investigated under joint AC and DC action [22]. Aguirre and co-workers [22] have reported on a kind of stationary parallel stripes oriented along the rubbing of the cells that occur in planar 5CB cells upon superimposed (combined) AC and DC electric fields. In the work presented here, we deal with the same NLC and report on pattern formation that looks similarly, but is formed by application of external DC field only. Our attention is concentrated onto the electrically-controllable change of the LDs induced in nematic 5CB in this way. The study is oriented to the achievement of electricaly-controlled optical diffraction by means of the formed LDs that is of interest for application in nematic-based diffractive-optic devices driven by low-voltage static electric field.

2. Experimental

Parallel-rubbed glass cells (the inner surfaces of the cell plates coated with ultrathin conductive layer of indium-tin-oxide (ITO) and polyimide) manufactured by E.H.C Co., Ltd.,Tokyo, Japan (trade name: KSRO-25/B111N1NSS Up/Low) with a thickness of (25 ± 0.2) μm were used in this work to form initially planar films of the NLC 4-*n*-pentyl-4′-cyanobiphenyl (5CB). The nematogenic material obtained from Merck was used without any special purification. At room temperature, 5CB has a stable nematic phase. This compound exhibits, on heating, the nominal phase sequence: Crystal – N (22.5°C), N – I (35.3°C), as reported by the manufacturer. The dipole moment of about 4 D determined by the cyano group is directed parallel to the long axis of the 5CB molecule. Being a birefringent material, the nematic 5CB is characterized by extraordinary and ordinary refractive indices $n_e = 1.706$ and $n_0 = 1.532$, respectively (at $\lambda = 633$ nm and 25 °C [23]. 5CB has a large positive dielectric anisotropy, $\Delta\varepsilon$ is about 10 at $T = 20$°C and $f = 1$ kHz [24]. In isotropic liquid phase, 5CB was injected into the cells by capillary forces. The formation of the NLC phase was examined with polarizing microscope by observing birefringence between crossed polarizers. The unidirectionally rubbed polyimide provided a strong planar alignment of the NLC having an overall orientation of the director along the rubbing direction. For comparative measurements, identical planar cells were filled with the NLC p-n-butyl-p-methoxyazoxy–benzene (BMAOB) that exhibits a nematic phase in the temperature interval 20°C – 74°C [25], as well as a negative $\Delta\varepsilon$ between -0.22 [25] and -0.25 [26].

DC voltage-dependent coherent light diffraction from the prepared films was studied by use of a collimated linearly-polarized ($> 10^4 : 1$) beam of He-Ne laser (wavelength $\lambda = 632.8$ nm, optical power ~ 1 mW, diameter of about 1 mm, divergence < 0.8 mrad, TEM_{00} spatial profile with a Gaussian intensity distribution). The laser output was circularly polarized, and the polarization direction of the beam (***P***) was selected by rotatable polarizer (Thorlabs LPVISB050-MP). The laser beam was directed nearly normally to the films. The diffracted light intensity was measured by a broad-aperture photodiode and computer-controlled system with automated data acquirement. The experiments were carried out at 28°C.

The morphology changes of the 5CB films upon DC voltage in the range 0 – 8 V were characterized by transmission optical microscopy (Zeiss NU-2 polarizing microscope). The microscope images were recorded by a Hitachi VK-C150ED video camera and computer. The diffraction pattern resulting from the propagating laser beam through the 5CB cells were visualized by a transversal imaging screen. Pictures were taken by 14 Mpx photocamera (Olympus VG-130-D-715, 4300 × 3200 pixels) in dark room.

3. Results and discussion

3.1. Domain morphology

Figure 1 shows the morphology in the studied 5CB films (initially planar) and its change as the applied DC voltage (V_{DC}) increases in the range 0 – 8 V, as displayed by polarizing microscope. Upon $V_{DC} > 4$ V – 5 V, well formed parallel stripes oriented along the direction of the rubbing of the cells were observed. The transversal size (the width) of these texture patterns varies somewhat from sample to sample, but was always larger than the

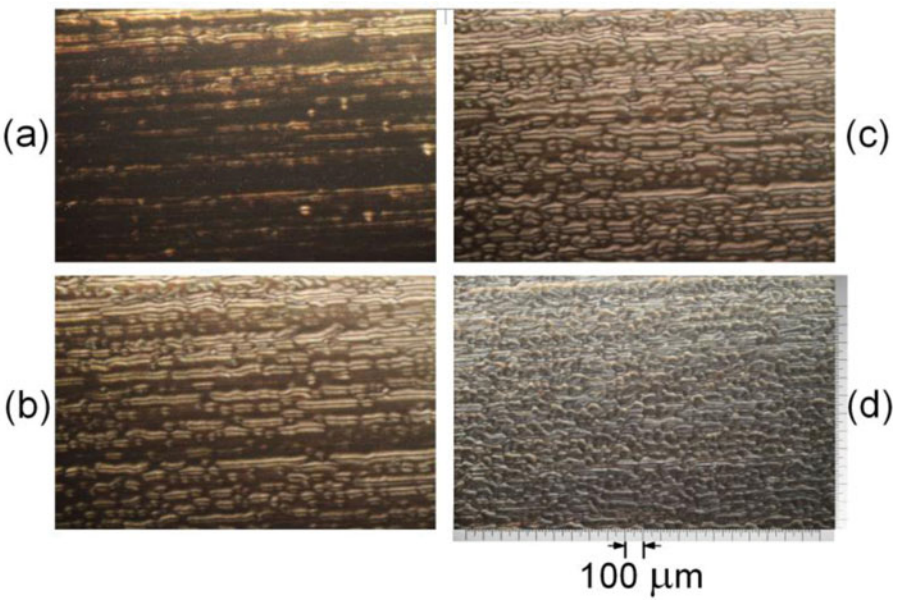

Figure 1. Evolution of the domain morphology of a planar cell with 5CB nematic. Micrographs were taken by crossed polarizers, the input light polarization was parallel to the rubbing of the cell (the rubbing direction of the cell plates was in the horizontal direction of the pictures). The DC voltage: 4 V (a); 4.5 V (b); 5.5 V (c); 6.5 V (d).

cell thickness (actually, more than twice as much as the cell gap). For the texture shown in Figure 1, an average width of about 52 μm was estimated. The texture formation was not uniform over the 5CB films. The length and the number of these longitudinal domains (LDs) vary in the different regions of the film suggesting some surface contribution to the domain formation.

The creation of LDs (Figure 1a) can be clearly viewed above a well pronounced voltage threshold. Previously, a distinct threshold for appearance of similar LDs has been reported for 5CB planar cells under the joint action of AC and DC voltages [22]. In our case of applying of pure DC voltage, the formation threshold was about 4 V. By increasing V_{DC} above the threshold (Figs. 1b, 1c), little changes of the morphology of the set of elongated patterns can be observed, mostly in their textural contrast. The latter increases substantially due to enhanced director field deformations. At V_{DC} higher than 6 – 6.5 V, the LDs fall into decay. Reasonably this is a result of the electrically-driven NLC reorientation above the Freedericksz transition toward to homeotropic alignment due to positive anisotropy of 5CB compound. Simultaneously, at higher V_{DC} field-induced hydrodynamic instability occurs in the 5CB films. This is accompanied by LDs deformations, but the LDs contours still remain (Figure 1d). By decreasing V_{DC} in the same range, from 8 V to 0 V, the textural changes of the 5CB films are repeated in reverse manner for the corresponding voltage values.

Following the orienting surface relief, the observed LDs (the static nematic director deformations) in the studied 5CB films exposed to a pure DC electric field consist of alternate bright and dark stripes parallel to the initial NLC alignment. By slight rotation of microscope stage, the brightness of the domain stripes is changed, indicating a presence of azimuthal deformations. The appearance and features of the LDs are similar to those of flexo-dielectric walls (FDWs) [27] having quadrupolar flexoelectric origin due to gradient electric field. The presence of weak anchoring, as well as an initial surface director tilt, are of importance for such FDWs [6, 27]. The Freedericksz transition (well detected for our samples) is a feature that clearly distinguishes the FDWs discussed here from the well known Vistin'–Pikin–Bobylev longitudinal flexoelectric domains (so-called flexodomains, FDs) in NLCs in planar-aligned cells [1,20,21,26,28–32]. Actually, in our case FDs are excluded due to the large positive dielectric anisotropy of 5CB. Further, we have found no significant change of the LDs spatial period with the applied DC electric field, in contrast to FDs in planar NLCs [1,20,21,26–29]. By applying a joint AC electric field with sinusoidal voltage amplitude comparable with the mixed DC voltage V_{DC}, the LDs we have observed were quickly erased.

The LDs observed here resemble the stationary parallel-striped patterns oriented along the rubbing of the cells, previously reported by Aguirre et al. for 5CB nematic in planar cells [22]. However, the latter texture (that also exhibits a well defined threshold and a voltage-independent spatial period) was found only under the joint action of DC and AC voltages. As such, a specific requirement for the formation of these patterns is the AC voltage application. A flexoelectric origin was suggested for these parallel stripes considered in [22], because their formation requires the presence of a DC field. Although longitudinal FDs are inhibited in planar NLCs with large positive dielectric anisotropy like cyanobiphenyls [1], the authors in [22] pointed out that the splay-bend director gradients near the electrode surfaces result in non-negligible flexoelectric polarization enough to initiate texture pattern. As noted in [22], since the LDs in 5CB planar cells appear at voltage much above the Freedericksz threshold voltage, the electrically-induced pattern formation occurs from a quasi-homeotropic state. It should be emphasized that stationary parallel domains in 5CB under DC electric field were

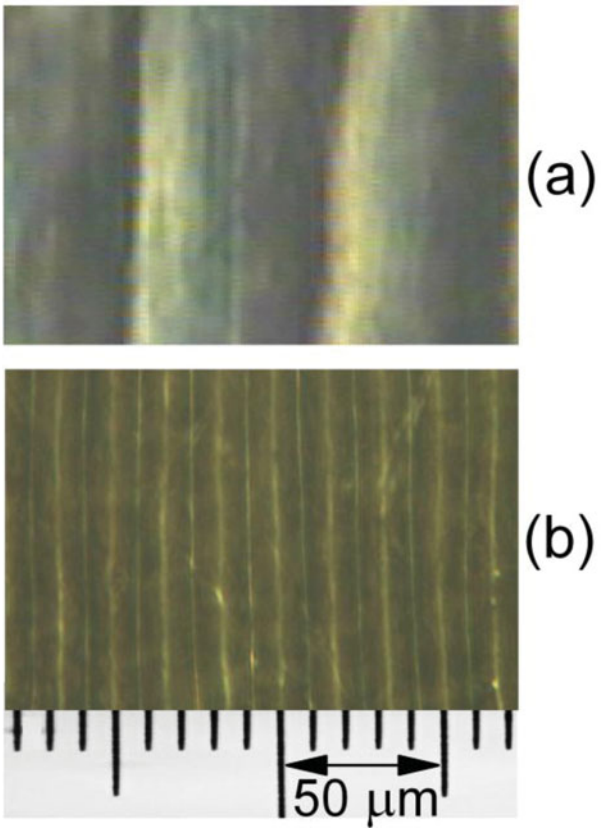

Figure 2. Micrographs of LDs: (a) FDWs in 5CB at 6 V; (b) FDs in BMAOB at 15 V in identical planar cells. Micrographs were taken by slightly uncrossed polarizers, the input light polarization was parallel to the rubbing of the cells (the rubbing direction of the cell plates was in the vertical direction of the pictures).

previously reported only in direction perpendicular to the orienting rubbing [4]. Such domains are surface-located and result from surface polarization.

The term "surface-located" is usually regarded to effects related to the boundary surface where, for instance, the surface polarization, weak anchoring, etc., could be present. The flexoelectric polarization is quite possible to play a significant role in the observed periodic instability as stated in Ref. [22]. In our case, the surface anchoring is relatively strong since the dielectric deformations in the 5CB cells we have studied start at 0.96 V_{RMS} as measured at 1 kHz frequency [33]. The observed director-gradient deformations are developed not at the surface but in the bulk, in a micrometer scaled region near the surface, where the electric field is non-homogeneous due to the presence of ions. The presence of ions (injection ions) was established by the measurement of current-voltage behavior of the same 5CB cells [33]. Further, the morphology of the LDs we have observed (Figure 2a), indicates that they are in the bulk, and are surface-located only in the region where they reach the top or the bottom surface of the NLC cell (both FDWs and surface declinations – the narrow dark stripes, are seen in Figure 2a, similarly to the observations in Ref. [6]). These features distinguish the FDWs from the FDs that are volume domains and are not associated to electric field gradient. For the sake of comparison, Figure 2(b) shows FDs formed in the NLC BMAOB in identical planar cell.

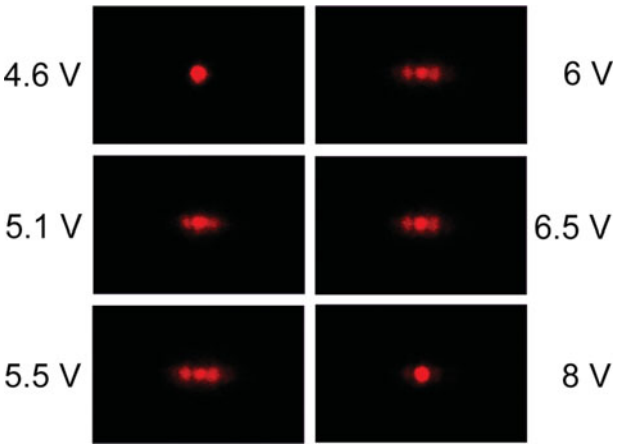

Figure 3. Diffraction pattern behind a planar 5CB cell (thickness 25 μm) illuminated with a He-Ne laser. The diffraction pattern was registered in transmission at various DC voltages as indicated. The polarization of the incident laser beam was along the rubbing direction of the cell. The pictures were taken under identical condition; cell-to-screen distance 15 cm.

3.2. Optical diffraction by flexo-dielectric LDs in 5CB planar cells under DC electric field

The DC electric field-induced director deformations in the form of spatially-periodic texture array of LDs in our initially planar 5CB nematic films can be practically applied. In fact, the set of stationary FDWs with well defined threshold and spatial period discussed in the previous SubSection, corresponds to an optical phase grating. The latter can produce optical diffraction when the 5CB films are illuminated by a highly coherent light beam (monochromatic and collimated). Indeed, in addition to the central peak (associated with the zero-th order diffracted light) two bright side-diffraction peaks occur from these periodic texture formations by illumination with a He-Ne laser beam when the voltage applied on the 5CB planar cells is above the formation threshold (Figure 3). The observed diffraction pattern (Fraunhofer type diffraction) looks like the one from a thin harmonic diffraction grating (see, for example [34]). Figure 4 shows a typical image of diffraction pattern as viewed at a long distance behind the 5CB cell. From the measured angular spacing of the features in the far-wave field diffraction pattern one can obtain the spatial frequency of the formed grating texture. The grating period we calculated in this way was $\Lambda \approx 46$ μm.

Figure 5 presents the first-to-zero order intensity ratio (η) for the diffracted light beams behind a planar 5CB cell, measured as a function of V_{DC}. As seen, above a certain V_{DC} value (in our case, $\sim$ 5 V) one can achieve a gradual change of η by V_{DC} applied to our planar cells with 5CB. Close to 5 V, in a short voltage range of about 1 V the variation of V_{DC} results in an abrupt change of η. Above 5.5 V, the variation of V_{DC} leads to a more gradual change of η. The electrically-controlled light intensity change of the observed diffraction light split resulting from Fraunhofer diffraction by LDs, as well as the sharp-maximum voltage-controlled curve for η, are attractive for applications, e.g. for stabilization of various processes by electric feedback, as well as for realization of electro-optic switches, active splitters and logical elements utilizing the light beam diffraction splitting (the physical separation of the beams). Reasonably, the specific V_{DC}-dependent curve for η is due to the electrically-induced change of optical anisotropy and electrically-driven reorientation of the nematic director by the applied electric field.

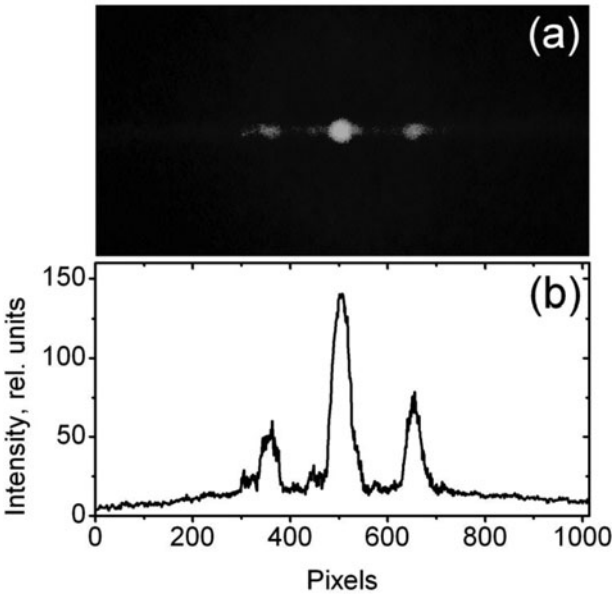

Figure 4. (a) As in Figure 3, but the diffraction pattern was registered in the far-wave zone: cell-to-screen distance 80 cm. The DC voltage was 6.5 V. (b) Digitized cross-sectional intensity profile of diffraction pattern shown in image (a).

The quantity η is indicative of the redistribution between the zero-th and the first diffraction orders, but can not be a measure for the diffraction conversion and efficiency, since this ratio does not really reflect the light energy conversion. In this context, we have to point out that lateral diffraction patterns of higher orders were still observed in the light diffracted behind the 5CB cells (Figure 6), but the intensity of such satellites of the strong triplet was rather weak. Also, the coherent light diffraction was accompanied by a coherent light scattering present as a speckle light cone around the central beam (seen in Figure 6). The scattered light (clearly observed as a halo around the zero-th order diffracted light) was strongest when the polarization ($\boldsymbol{P}$) of the input laser beam was parallel to the rubbing direction ($\mathbf{R}$) of the

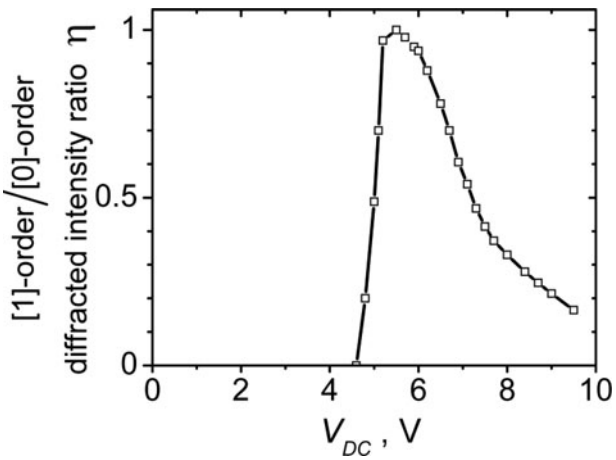

Figure 5. DC voltage-dependent intensity ratio η of the first-order diffracted light to the zero-order one (as measured under identical experimental conditions behind a 25 μm thick planar 5CB cell). The polarization of the incident He-Ne laser beam was parallel to the rubbing of the cell plates.

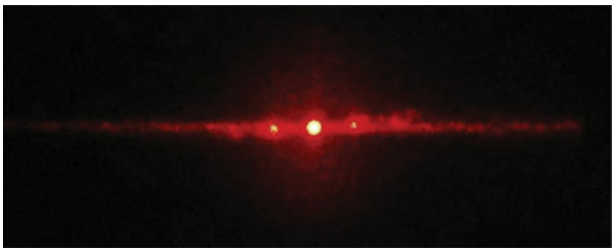

Figure 6. As in Figure 4(a), but the picture of diffraction pattern was taken by higher intensity of the incident laser beam.

cell plates (i.e., $\boldsymbol{P} \,||\, \mathbf{R}$), negligible in the orthogonal case ($\boldsymbol{P} \perp \mathbf{R}$), and with a gradually variable intensity in the intermediate situation. The polarization of the coherent light scattering follows $\boldsymbol{P}$. The same applies to the zero-th order coherent light diffraction. In contrast, the coherent light diffracted in the first-order is polarized principally in orthogonal direction. As for the peaks' intensity variation with $\boldsymbol{P}$ at a fixed V_{DC}, the triplet was strongest at $\boldsymbol{P} \perp \mathbf{R}$, had a lower intensity at $\boldsymbol{P} \,||\, \mathbf{R}$ (being reciprocal to the coherent light scattering intensity) and intermediate intensity at intermediate angle of $\boldsymbol{P}$. Since the optical background (the noise) from coherent light scattering can be avoided in the case $\boldsymbol{P} \perp \mathbf{R}$, this polarization configuration should be more advantageous for practical applications (in the main, the V_{DC}-dependent curve for η is similar as the one shown in Figure 5).

At this point it is probably interesting to be compared the diffraction by the pattern we have considered as formed in 5CB planar films with the diffraction by regular FDs, both induced by static electric field. For the purpose, we have conducted complementary measurements with BMAOB in identical planar cells and at the same geometry of the experiment. This NLC shows well developed FDs under the application of a DC field. Indeed, above a well defined threshold voltage (in our case about 11 V), well formed stable parallel stripes were viewed in the BMAOB cells by microscope (like those shown in Figure 2b). The spatial period of this phase grating decreases when V_{DC} increases, as reported in [20]. In contrast to the fixed diffraction triplet in Figures 3 and 4, the examined planarly-oriented BMAOB films exhibited multiple-peaks diffraction (Figure 7) with side-diffraction peaks better pronounced at higher V_{DC}. By increasing V_{DC}, the angular spacing between the central and the side diffraction peaks increases (Figure 7), and the zero-th order intensity gradually decreases (Figure 8). Further, a continuous redistribution of the peaks' intensity takes place with the variation of V_{DC}. As seen from Figure 8, the V_{DC}-dependent intensity of the zero-order diffraction achieved by FDs significantly differs from the specific dip-like one by FDWs considered here (also shown in Figure 8). As for the polarization characteristics of the observed diffraction through FDs in our BMAOB planar films, they also differ from these of the diffraction through FDWs in the planar 5CB films mentioned above. In fact, the variable-grating multiple-peaks diffraction by FDs behaves opposite to the diffraction through FDWs. Thus, the former one (together with the corresponding accompanying coherent light scattering) was not observed at $\boldsymbol{P} \perp \mathbf{R}$. By rotating $\boldsymbol{P}$, the light intensity diffracted by FDs increases to its maximum at $\boldsymbol{P} \,||\, \mathbf{R}$. Also, in contrast to the diffraction by FDWs, the polarization of all the light diffracted (and scattered) by regular FDs, repeats $\boldsymbol{P}$.

The V_{DC}-controlled diffracted light conversion (the curve for η, recall Figure 5) through the electrically-induced LDs in the considered 5CB planar films was fully reversible by ascending or descending V_{DC}. Since the diffraction conversion (and efficiency) are relatively high (by maximum conversion the intensity of the side peaks equals the intensity of the central peak),

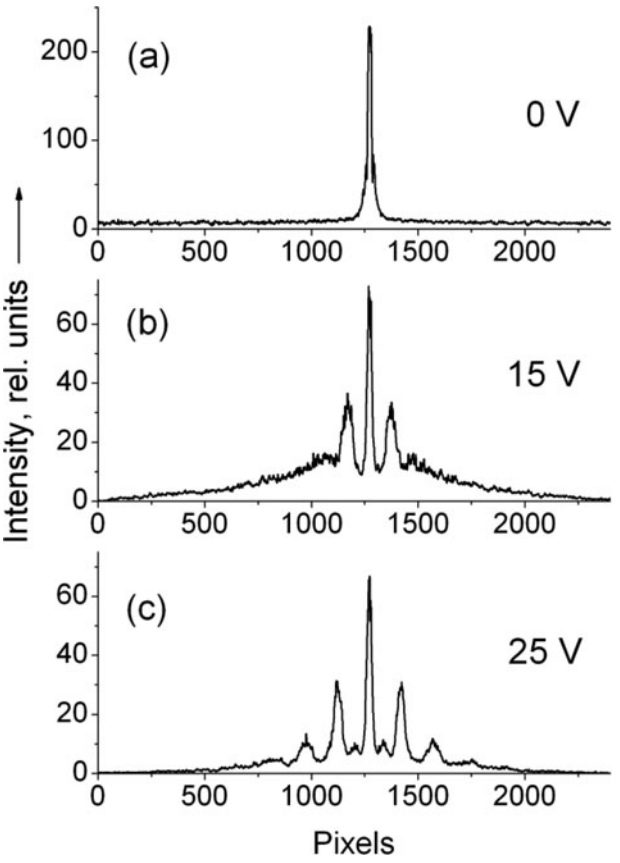

Figure 7. Cross-sectional intensity profiles of diffraction pattern registered behind a planar BMAOB cell (thickness 25 μm) illuminated with He-Ne laser whose polarization was along the rubbing direction of the cell. The pictures were taken under identical condition; cell-to-screen distance 15 cm. The applied DC voltage: 0 V (a); 15 V (b); 25 V (c).

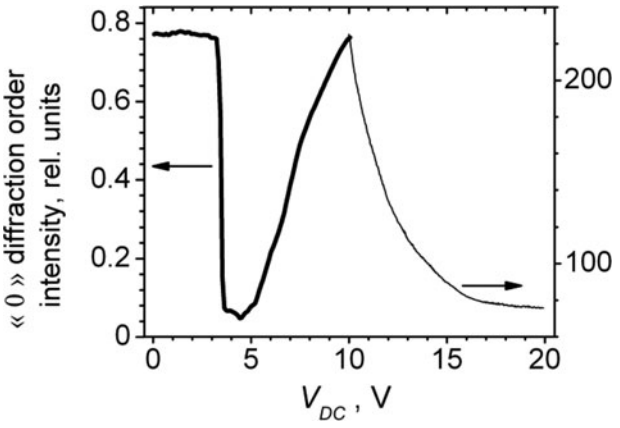

Figure 8. DC voltage-dependent intensity of the central peak in Figure 7 (zero-order diffracted light by FDs in BMAOB planar cell as compared to that by FDWs by 5CP planar cell (shown bold). Data obtained under identical experimental conditions; the polarization of the incident He-Ne laser beam was parallel to the rubbing of the cell plates.

this effect can be also exploited for efficient electro-optical control of laser beam intensity. Generally, the diffraction conversion (and efficiency) of the phase grating is restricted by both stray light and the high optical transmittance coefficient of NLC, in our case 5CB (the latter factor, however, is rather useful since it means a high resistance to high-power laser-induced damage). It should also be noted the diffraction from the 5CB films that occurs in reflecting geometry. As clearly observed in our experiment, the features of the backward diffraction duplicate these of the one in the forward direction (i.e. in transmission geometry), but with a considerably lower intensity.

As compared to other diffraction grating implementations in pure NLCs (without use of photo-active or electro-active agents), the main advantage of the grating effect by spatially periodic flexo-dielectric texture patterns considered here, is the low-voltage operation. Thus, in our case the magnitude of DC electric field strength ($\sim 2 \times 10^3$ V/cm) for proper light diffraction applications is at least 5 – 10 times lower than that necessary for gratings in low-frequency AC-excited thin layers of NLCs [35–37] and at least 10 – 20 times lower than the field strength for DC-activated gratings in NLC thin layers [9,13,14,38]. It may be also mentioned the LDs formed in planarly-aligned NLCs in the presence of a magnetic field that also have potential for some diffractive-optic applications, but need large magnetizing field strength. In particular, Hinov et al. [39] have recently reported periodic LDs in NLC of phenylbenzoates in planar cells exposed to a magnetic field (2 – 3 kOe). These LDs can be attributed to alignment-inversion walls oriented along the initial alignment of the NLC. In this case, the field-induced spatially-modulated optical anisotropy observed as highly regular LDs can be considered as a harmonic (sinusoidal) diffraction grating. Although such magnetically-driven LDs disappear in a few seconds after the magnetic field switching-on, they may still be useful for diffractive optics. However, in contrast to the electrically-driven LDs considered here, such a possible application is restricted by the complexity of the magnetic-field set-up.

It may be pointed out that the macroscopic configuration of the spatially-periodic LDs electrically-induced in planarly-oriented NLCs upon static electric field could be suitable to introduce electrically-driven macroscopic optical phase dislocations (singularities) in coherent optical waves propagating through such LDs ensembles. Thus, one can consider a manipulation of complex beam structures (such as dipoles, beam arrays, and vortices) propagating through NLC films under static electric field. Due to the negligible absorption and the huge optical nonlinearity of NLCs (with a highly nonlocal nature) [40–45] owing to large refractive index anisotropy, coupled with the electrically-induced collective molecular reorientation, similar planar textures (localized, but nonlocal) carrying striped distribution of electrically-induced optical phase pattern can be applied as low-powered spatial light modulators and other photonic devices for active control and manipulation of laser beams in coherent optics, non-linear optics, femtosecond photonics, as well as in singular optics and singular non-linear optics (for electro-optical spatio-temporal modification of laser wave fronts / laser pulses). In this context, the nonlocal response function [46] is important since the nonlocality will influence the minimum achievable spatial period of the texture and, hence, the spatial resolution and stability of a potential device based on spatially periodic flexo-dielectric texture patterns like these considered here.

4. Conclusions

Efficient control of diffraction splitting of transmitted laser beam is demonstrated as based on flexo-dielectric longitudinal domains (LDs) electrically-induced in planarly-oriented thin

nematic films upon low-voltage static electric field. In particular, we report on the electro-optic diffraction response of electrically-induced spatially-periodic array of LDs in planar cells with nematic pentylcyanobiphenyl (5CB). The light diffracted from such stationary phase grating texture in the plane of the 5CB cells is concentrated in only one central (zero-order) peak and two side (first-order) peaks whose intensity can be separately controlled by DC voltage in the range 4 V – 8 V applied on the cells. By that, about 30% of the diffracted intensity can be distributed into a single diffraction order as we obtained by highly coherent laser beam of nearly normal incidence and at wavelength of 632.8 nm. The diffracted light intensity alteration is achieved by DC electrically-controllable change of LDs textural contrast based on field-induced nematic director orientation deformations. Thus, we experimentally proved the ability of spatially modulated texture of flexo-dielectric LDs in planar nematics (that acts as an electrically-driven optical phase grating) for application in efficient low-powered diffractive electro-optic devices simply controlled by low-voltage DC electric field.

Acknowledgments

INERA EU project Research Potential (FP7-316309-REGPOT-2012-2013-1) is acknowledged, as well as the funding by the Ministry of Education and Science and National Science Fund of Bulgaria within the framework of research projects DFNI-TO2/10 and DFNI-TO2/18. The authors are extremely grateful to Academician Alexander Petrov and Assoc. Prof. DSc. Hristo Hinov from the Institute of Solid State Physics "Acad. Georgi Nadjakov", Bulgarian Academy of Sciences, for their valuable comments and suggestions, and for the helpful discussions.

References

[1] Pikin, S. A. (1991). *Structural Transformations in Liquid Crystals*, Gordon and Breach: New York.
[2] Blinov, L. M., & Chigrinov, V. G. (1994). *Electrooptic Effects in Liquid Crystal Materials*, Springer: New York.
[3] Buka, A., & Kramer, L. (Eds.) (1996). *Pattern Formation in Liquid Crystals*, Springer-Verlag: New York.
[4] Lavrentovich, O. D., Nazarenko, V. G., Pergamenshchik, V. M., Sergan, V. V., & Sorokin, V. M. (1991). *Sov. Phys. JETP*, *72*, 431.
[5] Kramer, L., & Pesch, W. (1996). In: *Pattern Formation in Liquid Crystals*, Buka, A., & Kramer L. (Eds.), Chapter 6, Springer-Verlag: New York, 221.
[6] Hinov, H. P., Bivas, I., Mitov, M. D., Shoumarov, K., & Marinov, Y. (2003). *Liq. Cryst.*, *30*, 1293.
[7] Barbero, G., & Lelidis, I. (2003). *Phys. Rev. E*, *67*, 061708.
[8] Barbero, G., & Lelidis, I. (2003). *Phys. Lett. A*, *311*, 242.
[9] Greubel, W., & Wolf, H. (1971). *Appl. Phys. Lett.*, *19*, 213.
[10] Carroll, T. O. (1972). *J. Appl. Phys.*, *43*, 767.
[11] Soffer, B. H., Boswell, D., Lackner, A. M., Tamguay, Jr., A. R., Strand, T. C., & Sawchuk, A. A. (1980). *Proc SPIE*, *218*, 81.
[12] Chavel, P., Sawchuk, A. A., Strand, T. C., Tanguay, Jr., A. R., & Soffer, B. H. (1980). *Opt. Lett.*, *5*, 398.
[13] Tanguay, Jr., A. R., Wu, C. S., Chavel, P., Strand, T. C., Sawchuk, A. A., & Soffer, B. H. (1983). *Opt. Eng.*, *22*, 687.
[14] Tangonan, G. L. (1985). *Electron. Lett.*, *21*, 701.
[15] Marcerou, J. P., & Prost, J. (1978). *Ann. Phys. (Paris)*, *3*, 269.
[16] Meyer, R. B. (1969). *Phys. Rev. Lett.*, *22*, 918.
[17] Petrov, A. G. (2001). In: *Physical Properties of Liquid Crystals: Nematics. EMIS Datareviews Series*, Dunmur, D. A., Fukuda, A., & Luckhurst G. R. (Eds.), Chapter 5, INSPEC- Institution of Electrical Engineers: London, 251.

[18] Buka, A., & Eber N. (Eds) (2013). *Flexoelectricity in Liquid Crystals: Theory, Experiments and Applications*, Imperial College Press: London.
[19] Elston, S. J. (2008). *Phys. Rev. E*, *78*, 011701.
[20] Marinov, Y., Petrov, A. G., & Hinov, H. P. (2006). *Mol. Cryst. Liq. Cryst.*, *449*, 33.
[21] Hinov, H. P., & Marinov, Y. (2009). *Mol. Cryst. Liq. Cryst.*, *503*, 45.
[22] Aguirre, L. E., Anoardo, E., Eber, N., & Buka, A. (2012). *Phys. Rev. E*, *85*, 041703.
[23] Li, J., Wen, C. H., Gauza, S., Lu, R., & Wu, S. T. (2005). *J. Disp. Technol.*, *1*, 51.
[24] Ratna, B. R., & Shashidhar, R. (1976). *Pramana*, *6*, 278.
[25] Blinov, L. M. (1978). *Electro- and Magnetooptics of Liquid Crystals*, Nauka, Moscow (in Russian); (1983) *Electro-Optical and Magneto-Optical Properties of Liquid Crystals*, Wiley: Chichester, U.K.
[26] Barnik, M. I., Blinov, L. M., Trufanov, A. N., & Umanski, B. A. (1978). *J. Phys. (Paris)*, *39*, 417.
[27] Hinov, H. P., & Vistin', L. K. (1979). *J. Phys. Paris*, *40*, 269.
[28] Bobylev, Y. P., & Pikin, S. A. (1977). *Zh. Eksp. Teor. Fiz.*, *72*, 369 [(1977). *Sov. Phys. JETP, 45*, 195].
[29] Bobylev, Y. P., Chigrinov, V. G., & Pikin, S. A. (1979). *J. Phys. Colloq. (Paris)*, *40*, C3–331.
[30] Schiller, P., Pelzl, G., & Demus, D. (1990). *Cryst. Res. Technol.*, *25*, 111.
[31] Kumar, P., & Krishnamurthy, K. S. (2007). *Liq. Cryst.*, *34*, 257.
[32] Krishnamurthy, K. S., Kumar, P., & Tadapatri, P. (2009). *J. Ind. Inst. Sci.*, *89*, 255.
[33] Hadjichristov, G. B., Marinov, Y. G., Petrov, A. G., Bruno, E., Marino, L., & Scaramuzza, N. (2015). *Mol. Cryst. Liq. Cryst.*, *610*, 135.
[34] Goodman, J. W. (2005). *Introduction to Fourier Optics*, 3rd edn., Roberts & Co.: Greenwood Village, Colorado, 78.
[35] Lu, S., & Jones, D. (1971). *J. Appl. Phys.*, *42*, 2138.
[36] Kashnow, R. A., & Bigelow, J. E. (1973). *Appl. Opt.*, *12*, 2302.
[37] Papadopoulos, P. L., Zenginoglou, H. M., & Kosmopoulos, J. A. (1999). *J. Appl. Phys.*, *86*, 3042.
[38] Soffer, B. H., Margerum, J. D., Lackner, A. M., Boswell, D., Tanguay, Jr., A. R., Strand, T. C., Sawchuk, A. A., & Chavel, P. (1981). *Mol. Cryst. Liq. Cryst.*, *70*, 145.
[39] Hinov, H. P., Vistin', L. K., & Marinov, Y. G. (2014). *J. Phys. Chem. B*, *118*, 4220.
[40] Peccianti, M., Conti, C., & Assanto G. (2003). *J. Nonlin. Opt. Phys. Mater.*, *12*, 525.
[41] Krolikowski, W., Bang, O., Nikolov, N., Neshev, D., Wyller, J., Rasmussen, J., & Edmundson, D. (2004). *J. Opt. B*, *6*, S288.
[42] Conti, C., Peccianti, M., & Assanto, G. (2004). *Phys. Rev. Lett.*, *92*, 113902.
[43] Henninot, J. F., Blach, J. F., & Warenghem, M. (2007). *J. Opt. A*, *9*, 20.
[44] Khoo, I. C. (2009). *Phys. Rep.*, *471*, 221.
[45] Izdebskaya, Y., Assanto, G., & Krolikowski, W. (2015). *Opt. Lett.*, *40*, 4182.
[46] Minovich, A., Neshev, D. N., Dreischuh, A., Krolikowski, W., & Kivshar, Yu. S. (2007). *Opt. Lett.*, *32*, 1599.